ELSEVIER

Polymer 40 (1999) 6265–6276

polymer

Morphology, deformation and failure behaviour of homo- and copolyimide fibres☆ 1. Fibres from 4,4′-oxybis(phthalic anhydride) (DPhO) and *p*-phenylenediamine (PPh) or/and 2,5-bis(4-aminophenyl)-pyrimidine (2,5PRM)

T.E. Sukhanova[a,*], Yu.G. Baklagina[a], V.V. Kudryavtsev[a], T.A. Maricheva[a], F. Lednický[b]

[a]*Institute of Macromolecular Compounds, Russian Academy of Sciences, Bolshoy pr.31, 199004 St.-Petersburg, Russia*
[b]*Institute of Macromolecular Chemistry Academy of Sciences of the Czech Republic, Heyrovsky sq.2, 162 06 Prague 6, Czech Republic*

Received 5 January 1998; received in revised form 18 December 1998; accepted 21 December 1998

Abstract

The morphology, deformation and failure behaviour of new high-performance polyimide (PI) fibres were examined by scanning electron microscopy (SEM), wide angle X-ray diffraction (WAXD) and tensile measurements. PI fibres were prepared from rigid aromatic diamines *p*-phenylenediamine (PPh) and 2,5-bis(4-aminophenyl)-pyrimidine (2,5PRM) and semi-rigid 4,4′-oxybis(phthalic anhydride) (DPhO) by wet-spinning of the *N,N*-dimethylacetamide solutions of their precursor poly(amic acids) in coagulation bath followed by thermal imidization at 400°C. The tensile properties and drawability of copolyimide (coPI) fibres were better than those of homopolyimides (homoPI). The improvement in fibre modulus and tensile strength of the coPI fibres can be explained by the microblock structure on the X-ray level and composed morphology on the macro level. Moreover, changes in the supermolecular structure and apparent fibril sizes, character of morphology, quantity of interfibrillar links, which affect the fracture mode were observed with the different composition of coPI.

Keywords: Morphology; Polyimide fibres; Failure behaviour

1. Introduction

For the development of new high-performance fibres, many different materials are used, one among them are the aromatic polyimides (PI). It has been found [1–5], that PI exhibit several valuable properties—good resistance to high temperatures and irradiation, high heat stability, maintaining good mechanical properties up to 500–600°C (only few other organic materials are competitive in this temperature range), satisfactory chemical resistance and noncombustibility, nonflammability, self-lubricity and a low coefficient of linear thermal expansion. This advantageous combination of technical characteristics makes it possible to consider PI as a promising class of polymer materials which can be used to solve some problems in the aircraft, car and aerospace industries, atomic energy industry, in the production of heat protective clothes and others. The high modulus and tensile strength of some PI fibres make them useful as reinforcing fibres in composite materials.

The first patents on fibres obtained from PI have been published by Irwin [6,7]. His studies were conducted with the polypyromellitimide fibres based on homo- and copolymers obtained by spinning from poly(amic acid) solutions (PAA). The best properties that resulted for such PI fibres were: a tensile strength of 2.4 GPa, an elongation of 4% and a Young's modulus of 92 GPa [7]. A few years later, several PI fibres were developed by Russian [8–11] and Japanese researchers [12–17].

Extensive investigations in the preparation of high-performance aromatic PI fibres have been summarised by Yang [2], Sroog [3] and Weinrotter [4]. It has been shown that in some cases the physical properties of the best of PI fibres exceeded values for Kevlar [18], for example, in the retention of tensile strength in air at 300°C and in the air-saturated steam at 200°C, in the chemical stability against

☆ Presented in part at the Europhysics Conference on Macromolecular Physics "Morphology of Polymers", July 17–20 1995, Prague, Czech Republic.

* Corresponding author.

0032-3861/99/$ - see front matter
PII: S0032-3861(99)00039-7

concentrated sulphuric acid at 85°C [14]. The oriented coPI fibres are comparable to Kevlar in the tensile strength of 3.3 GPa [14] and in elongation at break of 4.4% [14], but exceed in the Young's modulus of 180–205 GPa [8,9,12,13] (in comparison, maximum strength of 3.3 GPa has been obtained for Kevlar 129, an elongation of 4.5% for Kevlar 119, a modulus of 160 GPa for Kevlar 149 [18]).

The physical, mechanical and end-use properties of PI fibres depend strongly on their supermolecular structure and morphology, which is influenced by their composition, the way of production, and processing conditions. The crystalline structure of some PI fibres has been investigated in detail [1,12–14,19–22]. The literature contains some information about the morphology of PI fibres [19,20,23,24]; however, the outstanding properties of PI fibres require further explanation.

The main problems in the manufacturing of PI fibres are poor solubility and processability as well as the difficulties in synthesis. Moreover, the problem in their application is the brittleness of PI with high modulus, which may reduce the safety of their application. For these reasons, only a few PI have been used to produce the PI fibres in semi-commercial quantities up to now [1,2,4].

The general idea of molecular design for fibre-forming PI is creating the copolyimides (coPI) and PI blends as the possible way of the development of new materials with improved properties.

In the present series of papers, a variety of PI fibres made from rigid-chain and flexible- or semi-rigid chain homoPI and coPI with different compositions were studied. The possibility of changing the morphology and deformation behaviour of PI fibres by varying the monomer composition and blending was used.

The aim of this work was to disclose the structure of the homoPI and coPI fibres from DPhO-PPh and DPhO-2,5PRM with different composition on macro- and micro-level, to establish a relationship between structure and optimum properties, and propose the supermolecular structure models which can explain the mechanical behaviour of PI fibres.

2. Experimental materials and methods

2.1. Materials

The PI fibres were produced by a two-stage method [1]. The homoPI fibres were prepared by the polycondensation of an aromatic 4,4′-oxy-bis(phthalic anhydride) (DPhO) and *p*-phenylenediamine (PPh) or 2,5-bis(4-aminophenyl)-pyrimidine (2,5PRM). In the case of the copolymer synthesis, a mixture of diamines at a designated ratio with the added portion of DPhO was used. In the first stage, poly(amic acids) fibres (PAA) were prepared from 12(w/w)% solutions of pre-polymers in *N*,*N*-dimethylacetamide by wet-spinning process in coagulation bath (1:1 aqueous dimethylacetamide). The intrinsic viscosity of pre-polymer solutions range from $[\eta] = 2.8$ to 3.2 dl/g. The PAA fibres were drawn at a draw ratio of 3:1 in water at 50°C, washed and dried. In the second stage, the PI fibres were obtained by thermal imidization of PAA fibres at a constant length during the heating at 5–6°/min to 400°C and held at that temperature for 10–15 min. The chemical structures of the PI fibres studied are:

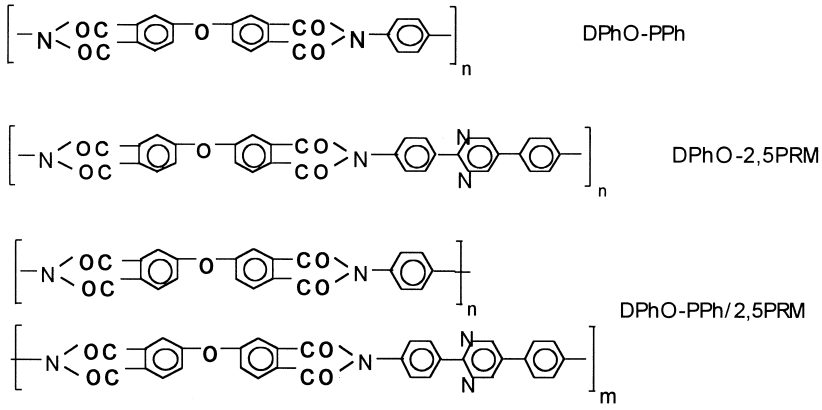

where $n/m = 80/20$; 60/40; 50/50; 20/80.

2.2. Scanning electron microscopy

The morphology of PI fibres was studied by scanning electron microscopy (SEM). A new morphological approach to mesomorphic systems, like some of the PI fibres was set up based on the permanganic etching of cut surfaces combined with peeling along the direction of fibre axis in various depths in order to disclose the structure well below the surface, fracturing under the loop-strength test, after tensile and flexural failure [23,24]. This allows one to reveal the morphology, to relate the difference in the mechanical properties with the morphological features and to propose the models of the supermolecular structure of the PI fibres.

Before the SEM observations, some PI fibres were etched by the permanganic etching method recommended by Olley and Bassett [25] for the observation of the fine details of the supermolecular structure. Recently, we

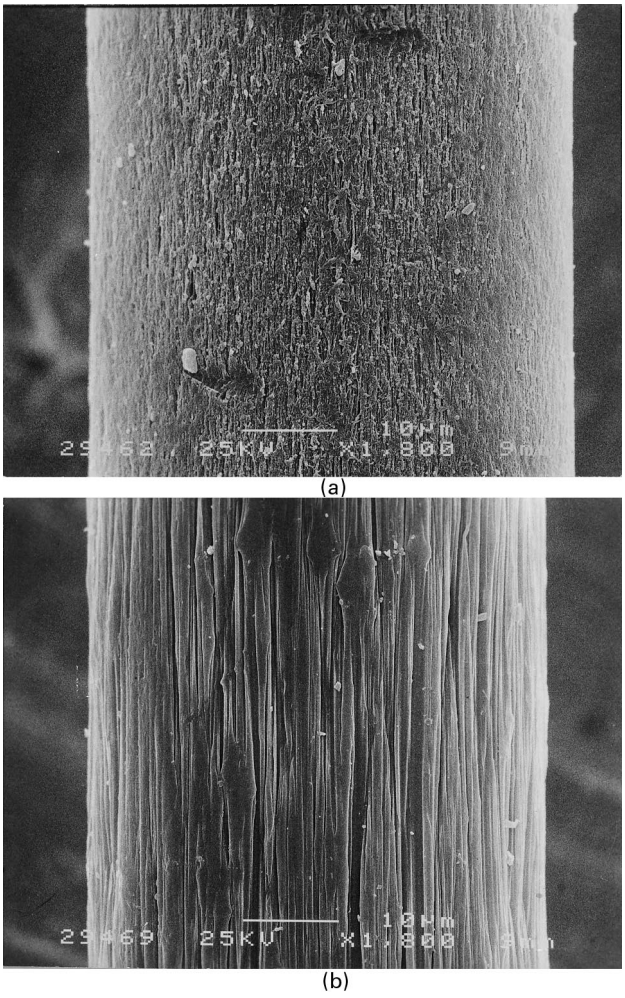

Fig. 1. SEM images of general view of homoPI fibres DPhO-PPh (a) and DPhO-2,5PRM (b); (a,b) 1.800 ×.

used this preparation technique to investigate the lamellar structure of fibre-reinforced PI fibre/isotactic polypropylene composites [26].

Samples were sputter-coated with a very thin layer of gold to prevent charging during imaging (SCD 050 ion-sputtering device, BALZERS, Switzerland) and examined on JSM-6400 (JEOL, Japan) SEM at 25 kV for magnifications from 400 × to 30 000 ×.

2.3. Wide angle X-ray diffraction

Wide angle X-ray diffraction (WAXD) analysis of PI fibres was carried out using a DRON-2 diffractometer and RKV-86 A camera with CuKα radiation and a Ni filter.

2.4. Mechanical testing

Comparison studies of the mechanical properties of the homo- and coPI fibres under investigation were carried out with fibre samples (ten for each deformation) 25 or 50 mm in lengths, which were axially extended to failure in a tensile machine (Instron 1125) with a speed of 10 mm/min. The average tensile strength was determined from the load-extention plots. Stress–strain relationships were obtained for the homoPI and coPI fibres with different composition of the diamine fragments.

3. Results and discussion

3.1. Surface topology

SEM analysis of the surface topology of the PI fibres under study shows that all fibres have a macroheterogeneous structure with differences in shape, dimensions of fibrils, size of fibrillar aggregates and pores. General view of fibres in Figs. 1a and b reveal very marked difference in a surface topology between the homoPI fibres studied. The structures appear to be of two general types.

High magnification SEM images of surface fragments of the homoPI and coPI fibres are shown in Fig. 2. The DPhO-PPh homoPI fibre has a very rough surface relief. There are a lot of spindle-shaped short microfibrils with pores and cavities 30–200 nm in width and 100 nm–2μm long between them in Fig. 2a. Globular aggregates which consist of globules, 30–100 nm in diameter, can also be seen on the fibre surface. The microfibrils themselves are 30–60 nm in diameter. Therefore, DPhO-PPh fibre exhibits the pore defect fibrillar structure on the surface. However, the DPhO-2,5PRM homoPI fibre has another type of morphology (Fig. 2d). This fibre consists of long, thick polymer bundles which are fibrillated into ribbons with widths ranging from about 30 nm up to a few micrometres. We have not observed pores on the surface, but there are some defects which look like extended cavities between the bundles in Fig. 2d.

When the surface of coPI fibres are observed, we see the changes in morphology which depend on the composition. The coPI fibre with a composition of 80/20 in Fig. 2b shows slightly thicker fibrils, 60–100 nm in diameter, than the homoPI fibre of DPhO-PPh, and larger globular aggregates on the surface. For a fibre with a composition of 50/50 in Fig. 2c, as well as with a composition of 60/40, we cannot resolve the fibrillar morphology on the surface. It appears to be smooth under low magnifications. A lot of globular aggregates covered the fibre surface with the diameter ranging from about 20 to 500 nm under high magnifications.

3.2. Internal structure of PI fibres

For the visualisation of the internal morphology, the fibres embedded in the thermoplastic matrix, were cut longitudinally and transversally at room temperature using a glass knife. The cut surfaces were then etched by the permanganic etching method.

Fig. 3a is a longitudinally cut surface of the DPhO-PPh homoPI fibre. Skin-core morphology is clearly seen on this micrograph. The transverse cut surface of the DPhO-PPh homoPI fibre and matrix is shown in Fig. 3b. The fibre

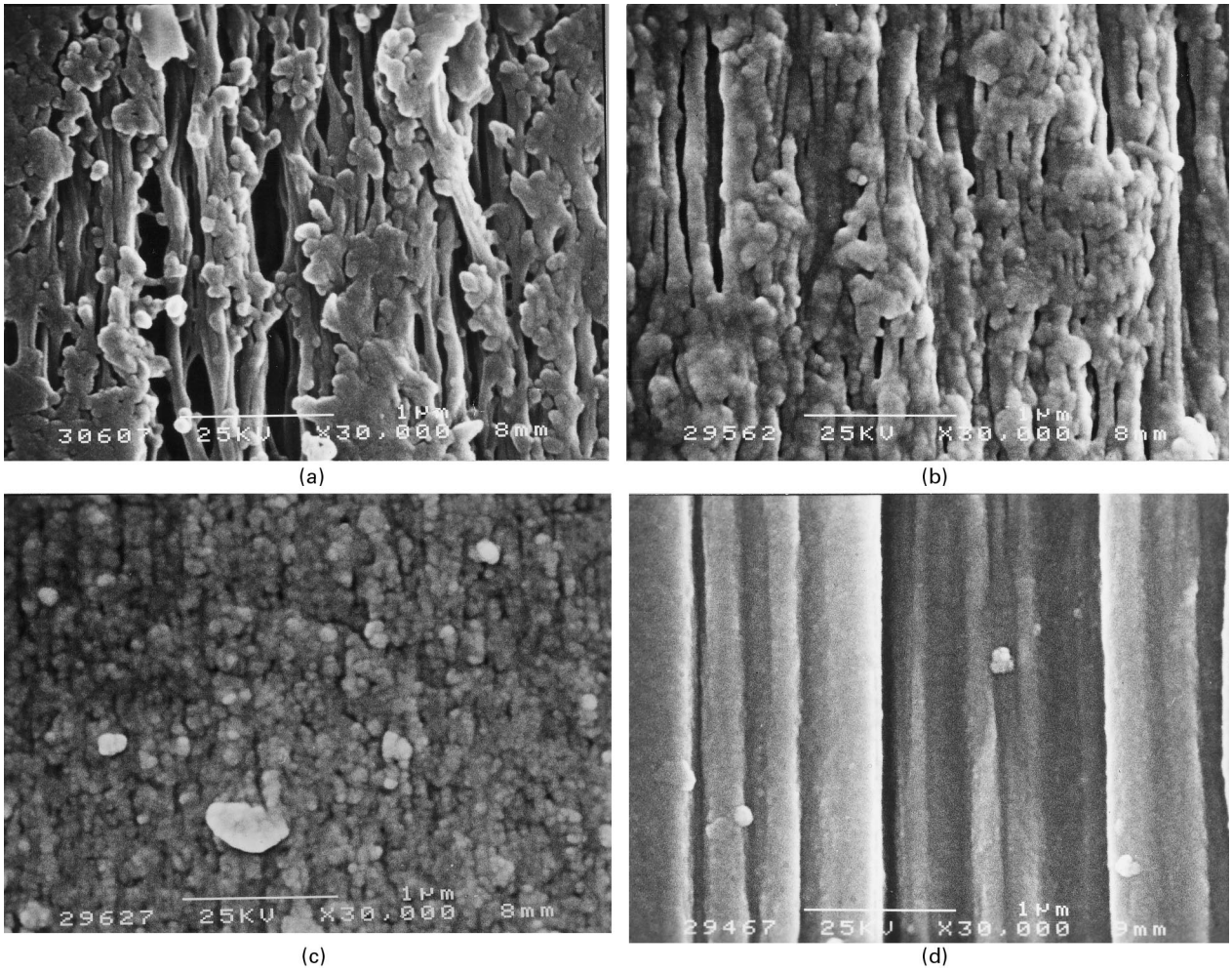

Fig. 2. High magnification SEM images of surface fragments of homo- and coPI fibres: (a) DPhO-PPh; (b) DPhO-PPh/2,5PRM (80/20); (c) DPhO-PPh/2,5PRM(50/50); (d) DPhO-2,5PRM.

exhibits a skin-core morphology with a feasible porous skin of 2–4.5 μm in thickness and a more dense core. There are a lot of small and large pores from 50 to 200 nm in size in the cross-section of fibre which are concentrated in the skin region. It should be noted that some of these pores arose during the etching process due to the different rates of etching in the defective and amorphous regions within the fibre. The skin and the core appear to be composed of fibrils as the fibrils are 0.5–1.0 μm in diameter in the core and 3–4 μm in diameter in the skin. These fibrils are composed from microfibrils 30–60 nm thick, consistent with that seen in Fig. 3b.

Fig. 3c and d–fare longitudinal and transverse cut surfaces of the DPhO-2,5PRM homoPI fibre, which show another type of morphology. The fibre cross-section in Fig. 3c exhibits a ribbon-like morphology with the bundles of ribbon cross-sections with the dimensions of about 0.5–1.0 μm × 1.0–1.5 μm and a multiple cracking. This is due to the splitting during the transversal cutting, with the cracks running around these bundles. Every bundle consists of thin ribbons 20–30 nm thick which are seen in Fig. 3f. The homoPI fibre of DPhO-2,5PRM has a ‘wood-like’ appearance of the cross-section (Fig. 3e). There is no skin in the transverse cut surface, but a thin surface layer about 0.2–0.5 μm seems to be less ordered than the core (Fig. 3f). A ribbon-like morphology is characteristic for this fibre. This structure appears to consist of a close-packed arrangement of very long ribbon-shaped structural entities about 20 nm in thickness and 1–3 μm in width. Fig. 3c–f show the different fragments of the cross-section of a single DPhO-2,5PRM fibre. Various degree of microfibrillar packing (aggregation) can be seen in one fibre on the cross-section and along its length, but the main character of morphology is the same.

Additional information on the internal fibre structure was obtained by observations on peeled fibre surfaces. Fig. 4 shows the peeling of the homoPI and coPI fibres. DPhO-PPh fibre in Fig. 4a peeled with difficulties due to its brittleness (elongation at break 1.5%). A little part of the fibre skin, about 1 μm was only peeled. The coPI fibres in Figs. 4b and c failed in the peeling revealed continuous ribbons and many partially separated thin fibrils about 300 nm in

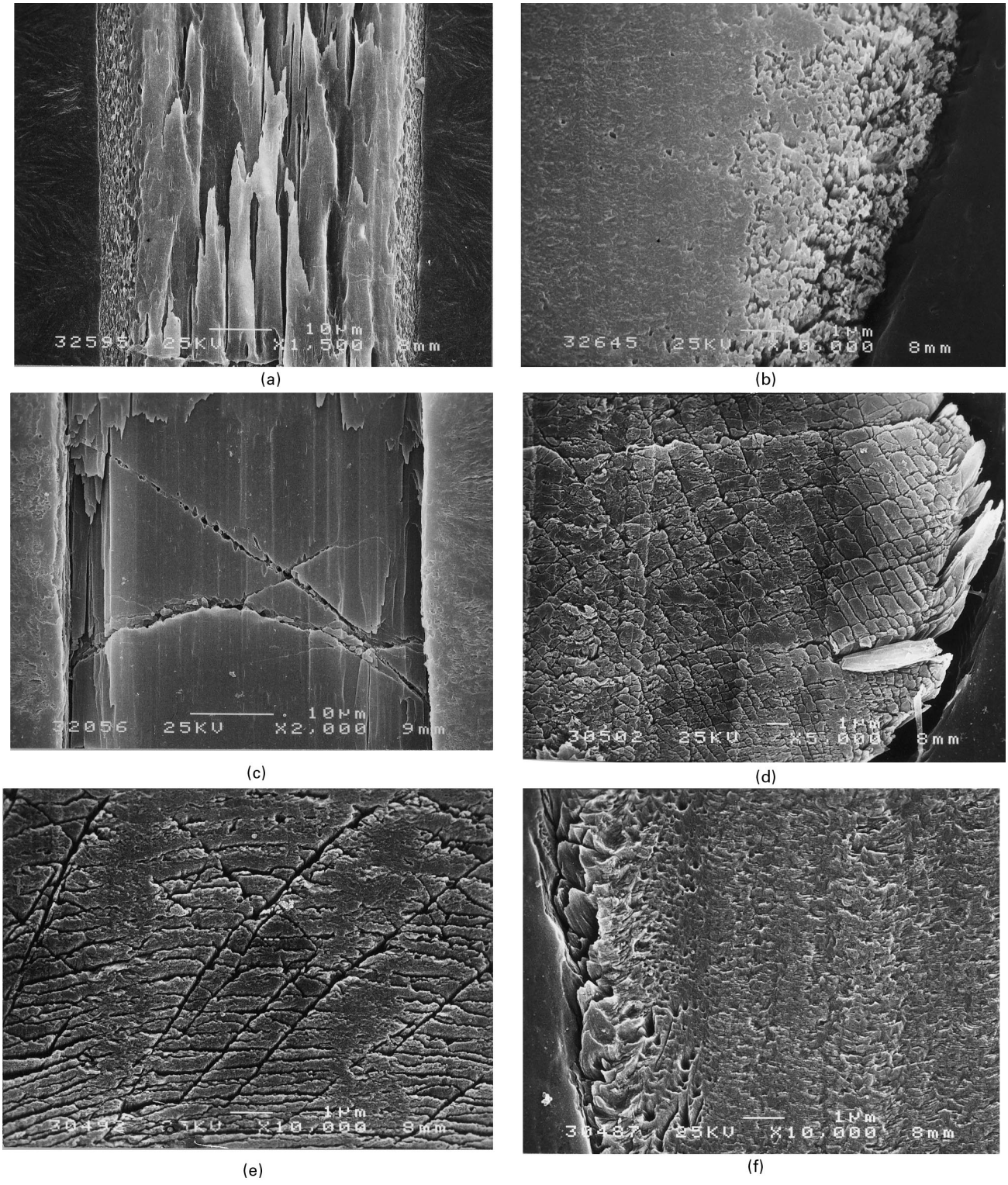

Fig. 3. SEM micrographs of the etched cut surfaces of homoPI fibres in longitudinal (a,c) and transversal (b,d–f) directions: (a,b) DPhO-PPh, (c–f) DPhO-2,5PRM.

diameter. Such tear off fibrils coil into spirals and helices (more pronounced in Fig. 4b), indicating that there are plastic strains inherent within these fibrils prior to the release of the load and form periodic plastic zones in compression after the fibre snaps back. The presence of the plastic deformation features shows that the coPI fibres have more ductility than the homoPI fibre of DPhO-PPh.

Electron microscopical observations of peeled surfaces

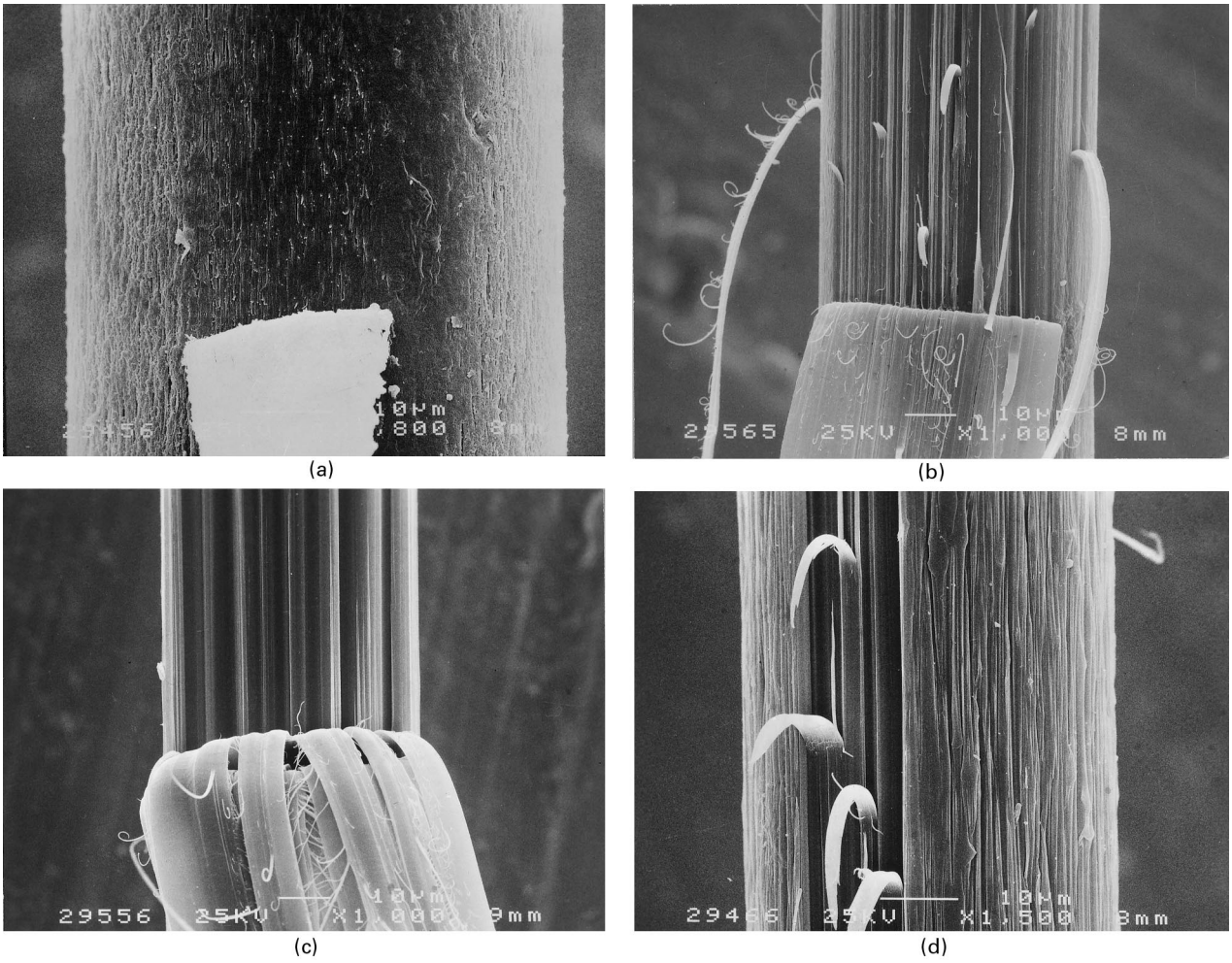

Fig. 4. SEM images of peeled fibres (general view) of homo- and coPI fibres: (a) DPhO-PPh; (b) DPhO-PPh/2,5PRM (80/20); (c) DPhO-PPh/2,5PRM (50/50); (d) DPhO-2,5PRM.

under high magnification in Fig. 5 indicate that the internal fibrillar morphology in homoPI are arranged differently than those in coPI fibres. HomoPI fibre of DPhO-PPh (Fig. 5a) exhibit short thick fibrils 100–200 nm in diameter. One can observe on the peeled surface several bright points (about 15 points in Fig. 5a), which correspond to the ends of the torn fibrils. They relax after stretching during the peeling and become spherical entities protruding from the peeled surface.

However, the homoPI fibre of DPhO-2,5PRM (Fig. 5d) exhibits a very smooth peeled surface with a number of lines spaced parallel to the fibre axis. This means that this fibre has a densely-packed layered ribbon-like morphology. Few bright globular points on the micrograph correspond to the torn microfibrils. Several ends of destroyed microfibrils are concentrated at the place where the ribbon was broken (bottom left in Fig. 5d). Cracks readily pass between the ribbons in the longitudinal direction. Long crack propagation does occur.

DPhO-PPh/2,5PRM coPI fibre with the composition 80/20 in Fig. 5b has a fibrillar morphology with spindle-shaped fibrils of 30–100 nm in diameter and 10 μm long. There are about 200 bright points on the micrograph. Therefore, the quantity of interfibrillar molecules is higher than in the homoPI. The fibre exhibits the unique ‘strand of beads’ fibrillar morphology. On the peeled surface of the coPI fibre with a composition of 50/50, we observed very long fibrils 30–70 nm thick also with ‘strand of beads’ morphology (Fig. 5c). These beads were of 15–30 nm in diameter. Such a type of fibrillar morphology was observed only for the copolymer fibres of DPhO-PPh/2,5PRM with the DPhO-PPh content from 80% to 50%.

These results have shown that the peeling is a very useful preparation technique for the visualization of the inner morphology of fibres as well as the interfibrillar cogesion. From the analysis of the peeled surfaces we can calculate the fibril thickness, quantity of destroyed microfibrils and interfibrillar links and estimate the cogesion between the supermolecular entities. The micrographs in Fig. 5 show that the ductility and lateral strength of the coPI fibres are higher than that for the homoPI fibres and also that the coPI are not as well oriented as the homoPI.

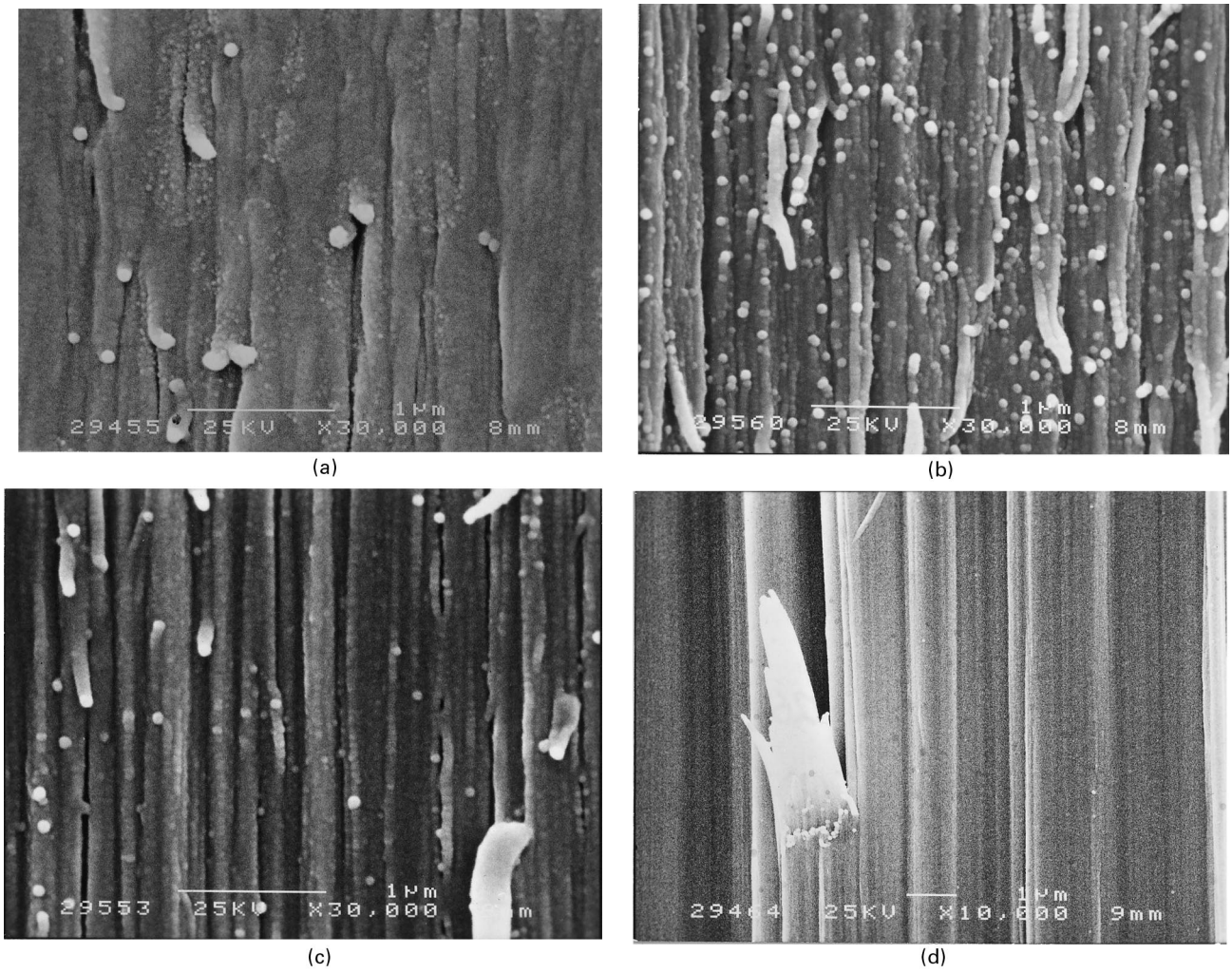

Fig. 5. High magnification of peeled surfaces of homo- and coPI fibres: (a) DPhO-PPh; (b) DPhO-PPh/2,5PRM (80/20); (c) DPhO-PPh/2,5PRM (50/50); (d) DPhO-2,5PRM.

3.3. Failure and deformation behaviour of PI fibres

Fig. 6 illustrates the microscopic failure processes of individual fibres that had been fractured under bending. Failure, transverse to the fibre axis, can occur only in the DPhO-PPh homoPI fibre (Fig. 6a). The crack follows a pass around chain ends and the ends of the fibrils inherent in the fibre. When the fibre is torn off by bending, sharply pointed tips are formed at the broken end of a fibre. This fibre does not fibrillate extensively, which implies that its lateral strength is higher than the longitudinal one.

Fig. 6d reveals that DPhO-2,5PRM homoPI fibre fail in bending by axial splitting 70–150 times their diameter *D* along their length. Crack propagation can readily occur parallel to the fibre longitudinal axis because only this requires the interfibrillar rupture. We have observed that the PI fibres split the lengths and the tendency for splitting decreases when the content of 2,5PRM in the coPI decreases from 100 to 20 mol% (Fig. 6c and 6b). The fibre with a composition of 50/50 also split along their length, but half of the fibre is deformed without splitting, the buckling on the surface was only observed. For these failures, the average angle between the two parts of the fibre before the delamination of outer layers and splitting was 100–110°. This mode of fracture is due to the high elastisity of the coPI fibre with a composition of 50/50 in comparision with the homoPI fibres as well as better interfibrillar contacts.

Examination in the SEM of the coPI fibres, bent through varying degrees, shows a characteristic banding restricted to the inner surface of the loop. At the composition 50/50, the bands appear to be singular and evenly distributed around the curve. These are the kink bands, which arise on the surface and propagate from the skin towards the fibre axis like in Kevlar fibres [27].

The electron microscopic observation reveals that there are two kinds of cleavage planes, one being perpendicular to the fibre axis and the other parallel to the fibre axis. The fibre with the composition 80/20 in Fig. 6b reveals combined failures: partial skin failure transverse to the fibre direction,

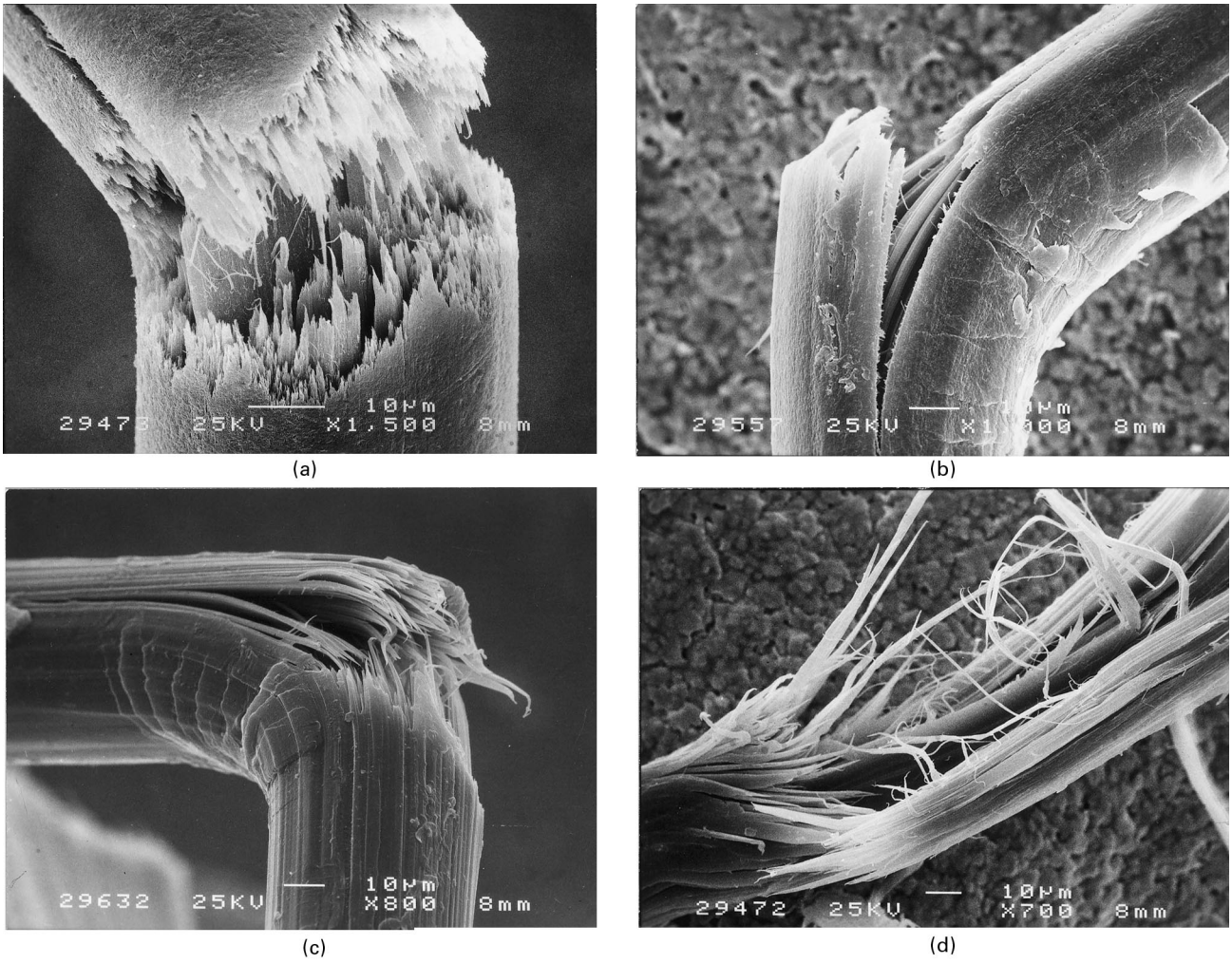

Fig. 6. Typical fracture surfaces of homo- and coPI fibres: (a) DPhO-PPh; (b) DPhO-PPh/2,5PRM (80/20); (c) DPhO-PPh/2,5PRM (50/50); (d) DPhO-2,5PRM.

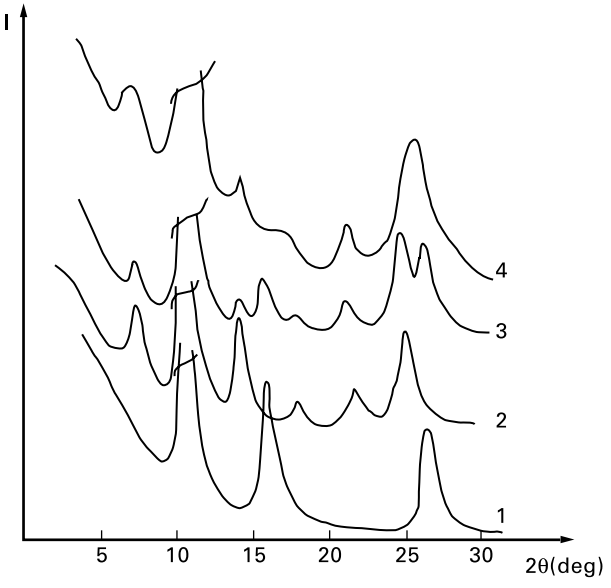

Fig. 7. X-ray diffractograms of meridional regions obtained from PI fibres: (1) DPhO-PPh; (2) DPhO-2,5PRM; (3) blend of DPhO-PPh/DPhO-2,5PRM (50/50); (4) coPI of DPhO-PPh/2,5PRM (50/50).

which do not completely circumvent the fibre and longitudinal crack propagation inside, but it is not so extensive as in previous ones.

The fracture mechanism is dependent upon the fibre structure. The microfibrils provide connectivity between the large fibril bundles. It is highly probable that the tolerance to bending and improvement in the thermomechanical properties [28] result from the peculiar ‘strand of beads’ fibrillar morphology of the coPI fibres studied.

3.4. Microstructure of fibres

Investigation of the crystalline structure of PI fibres obtained from DPhO-PPh and DPhO-2,5PRM homoPI, DPhO-PPh/2,5PRM coPI and DPhO-PPh/DPhO-2,5PRM blends of different compositions was carried out in detail. It has been shown recently [19–21] that the main information on the microstructure of insoluble coPI can be obtained by the analysis of the meridional reflections of the oriented samples, using the X-ray diffraction patterns.

For the homoPI fibre of DPhO-PPh, the diffractogram

Table 1
Measured values of interplane distance d (nm) from meridional reflections of X-ray patterns homoPI and coPI fibres from DPhO dianhydride and PPh (n) and 2,5PRM (m) diamines

Mole ratio (n/m)	d_1	d_2	d_3	d_4	d_5	d_6	d_7	d_8	d_9
100/0	—	—	0.820	—	0.560	—	—	—	0.338
80/20	—	—	0.820	—	0.553	—	—	—	0.334
60/40	—	—	0.818	—	0.560	—	0.420	—	0.380
50/50	—	—	0.820	—	0.520	—	0.410	—	0.340
50/50 (blend)	2.44	1.237	0.825	0.618	0.530	0.502	0.418	0.350	0.334
20/80	—	1.249	0.815	0.623	—	0.500	0.420	0.356	—
0/100	2.452	1.251	0.818	0.627	—	0.501	0.418	0.358	—

(Fig. 7, curve 1) exhibit reflection at the Bragg angle $2\theta = 11°$ (with strong intensity) and two reflections at $2\theta = 16°$ and $2\theta = 26°$ (with medium intensity) related to the periodicity along the polymer chains. In the case of homoPI fibre DPhO-2,5PRM (Fig. 7, curve 2), multiple sharp meridional reflections at $2\theta = 7°$, 11° (very strong), 14°, 18°, 21° and 25° were observed. The existence of clear meridional reflections demonstrate a regular arrangement of the polymer chains along the fibre axis in both homoPI. The average length of the ordered regions in DPhO-PPh homoPI fibre is $L \sim 120–125$ Å, at the same time in DPhO-2,5PRM homoPI fibre, these domains are larger ($L \sim 160–180$ Å). For meridional reflections at $2\theta = 11°$ (with spasings $d = 8.18$ Å and $d = 8.2$ Å), the half-width is $\Delta\varphi = 48–50'$ for DPhO-PPh and $\Delta\varphi = 24'$ for DPhO-2,5PRM homoPI fibres. This indicates that the macromolecules are more oriented in the homoPI fibre of DPhO-2,5PRM.

A comparison of the interplane distances of homoPI, coPI fibres with the composition 80/20, 60/40, 50/50 (Fig. 7, curve 4) and 20/80, and blend with the component ratio 50/50 (Fig. 7, curve 3) are listed in Table 1.

The diffractogram of fibres based on the PI blend DPhO-PPh/DPhO-2,5PRM with the component ratio 50/50 (Fig. 7, curve 3) exhibits the reflections of both homopolymers. The diffraction pattern also shows a limited number of well defined several order (00l) reflections for coPI fibres with the component ratio $m/n = 50/50$ (Fig. 7, curve 4), which indicate the microblock structure of coPI [19,21,23]. The average length of the microblocks evaluated by the analysis of the half-width of the reflections is found to be 4–5 monomer units of DPhO-2,5PRM ($L \sim 110–125$ Å). Low intensity and diffuse character of the reflection at $2\theta = 16°$, which correspond to the (006) reflection plane of the homoPI DPhO-PPh in the copolymer macromolecules, is due to the statistical dispersion of the microblock length of DPhO-PPh (2 or 3 monomer units). In this case, the microblocks of DPhO-PPh act as flexible spacers between the more rigid and large microblocks of DPhO-2,5PRM.

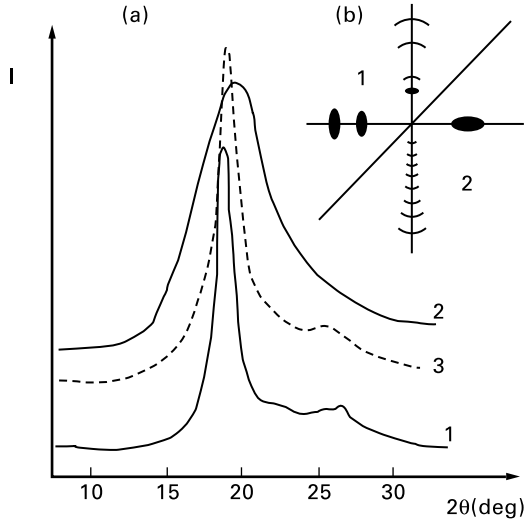

Fig. 8. X-ray diffractograms of equatorial regions (a) and schematic representation of X-ray patterns (b) of homo- and coPI fibres: (1) DPhO-PPh; (2) DPhO-2,5PRM; (3) DPhO-PPh/2,5PRM (60/40).

Table 1 shows the Bragg spacings of the meridional region of the X-ray diffractograms for the DPhO-PPh/2,5PRM coPI fibres with the component ratio $m/n =$ 80/20 and 20/80. One can recognize that in the first case (80/20), the reflections (00l) of the DPhO-PPh homoPI are well-defined; however, for the component ratio 20/80, the reflections of the DPhO-2,5PRM homoPI are more pronounced. It is interesting that in the coPI fibre with the composition 80/20 the average length of the ordered regions of DPhO-PPh is $L \sim 110$ Å, but the DPhO-2,5PRM homoPI did not manifest in coPI. At the same time, the DPhO-PPh homoPI reflections did not appear in the fibre with the composition 20/80.

The analysis of the equatorial regions of diffractograms indicates that the order of the intermolecular packing in the transversal direction in the DPhO-2,5PRM homoPI fibre is lower than that in the DPhO-PPh homoPI and coPI fibres with the component ratio 50/50 (Fig. 8a). HomoPI fibre of DPhO-PPh exhibits sharp reflection at the Bragg angle $2\theta =$ 18–20°; however, homoPI fibre of DPhO-2,5PRM has a more diffuse and more arched reflection at $2\theta = 16–23°$. It can be concluded that DPhO-PPh homoPI fibre has a more dense mutual packing of macromolecules than mesomorphic packing of DPhO-2,5PRM homoPI fibre. It has been supposed [29] that the shift placement of macromolecules exists in the pyrimidine containing PI which result in the mesomorphic type of the structure appearance.

Fig. 8b is a schematic representation of X-ray patterns obtained from the DPhO-PPh fibre (1) and the DPhO-

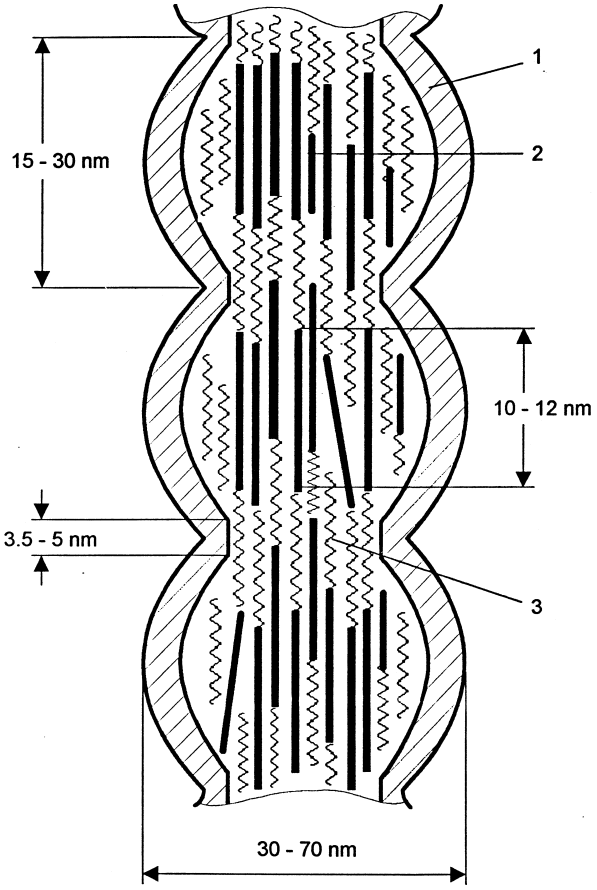

Fig. 9. Rough sketch of a hypothetical structure of fibrils in coPI fibres as revealed by SEM: (1) a conductive gold layer (about 7 nm thick); (2) the 'bead-like' portion of the fibril; (3) the 'rod-like' portion of the fibril (see the text).

2,5PRM fibre (2). It can be recognised that the angle of disordering along the chain axis is about 20–30° for DPhO-PPh and 10–20° for the DPhO-2,5PRM homoPI fibres, which supports the greater orientation of the DPhO-2,5PRM macromolecules than the DPhO-PPh ones.

4. General discussion

On the basis of the data given earlier, we can define several types of morphological organization in the PI fibres studied: spindle-shaped short fibrils for DPhO-PPh fibre, long ribbon-like fibrils for DPhO-2,5PRM fibre and peculiar 'strand of beads' fibrils for the coPI fibres with the component ratio from 80/20 to 50/50. The gradual change in the fibrillar morphology, supermolecular structure, thickness and homogeneity of the skin as well as in a radial heterogeneity were observed in the copolymer fibres with a different mole ratio of the components.

The structure of coPI fibril for DPhO-PPh/2,5PRM fibre with the composition 50/50 is schematically illustrated in Fig. 9. When the gold layer (1) about 7 nm thick, covering the fibre surface is taken into account, we can bear some direct relation to the parameters of the microblock structure which was observed by X-ray investigations. The 'bead-like' portion of fibrils (2) measured by SEM is about 15–30 nm long and 30–70 nm thick. It may be suggested that the central part of each bead comprised of the rigid microblock which is formed from 4–5 monomer units of DPhO/2,5PRM ($L \sim 10$–12 nm, bold line). The beads are connected by more flexible blocks of DPhO-PPh (3) ($L \sim 3.5$–5 nm, zigzag line) with the resulting formation of the 'strand of beads' fibrillar morphology in coPI fibres. It should be mentioned that this picture depicts only hypotetically the fibrillar structure of coPI fibres disclosed by our study.

Such unique fibril shape in coPI fibres may be treated as mixed morphologies, resulting probably from a phase separation that occurred before crystallization. During the coPI fibres formation, some portion of the copolymer precipitates from solution and creates the amorphous beads surrounding the central thread.

Mixed morphologies consisting of both needle-shaped crystals and spherical beads had been prepared by Waddon and Karasz, by evaporation of solvent in moist air during the crystallization process of the semi-rigid aromatic PI BTDA 3,3′-DDS [30]. They supposed that for the specimens that display both crystals and beads in the final morphology, crystallization had simply been arrested by absorption of water, evaporation of the solvent and consequent phase separation. As a result, some part of the polymer was amorphous and adopted a 'bead-like' morphology on the scale of 30–200 nm. Somewhat similar results have been published previously by Livingston [31] with interfacially polymerized 610 nylon precipitated from aqueous hexafluoropropan-2-diol by cooling. The opaque spherical particles of an average diameter of 20 nm and particles shaped like extended-chain crystals (the rods about 0.2 μm long) were observed simultaneously.

X-ray investigations show that both the homoPI and coPI fibres studied exhibit mesomorphic structure with various degree of orientation and mutual packing of macromolecules. It has been shown [19–21] for coPI fibres from the pyromellitic dianhydride and diamines with varying rigidities that the microblock structure is formed in these systems. The PMR spectra of PAA solutions of copolymers established that the microblock structure arise during polycondensation [21]. The comparison of the intensities of PMR spectra signals enabled the evaluation of the mean block lengths: 4–5 units for rigid blocks and 5–6 units for flexible blocks in coPI fibres and films with 50/50 mole ratio of the components. This structure retained after annealing of the oriented samples at 400–500°C. This result was obtained for the rigid pyromellitic dianhydride.

In the case of DPhO dianhydride, there is an oxygen atom in this fragment of the PI chain which resulted in some conformational mobility of the polymer chains. Conformation calculations reveal [22] that for the PI with DPhO dianhydride and rigid diamines PPh, benzidine (B) and

2,7-diaminefluorene (Fl) the flexion distortion is small and macromolecules exhibit a number of rod-like conformations.

In our case, the possibility for coexistence a lot of rigid quasi-helical chain conformations is correlated to the identity period calculated for 2 monomer units from the X-ray data: $c = 33.8 \pm 0.1$ Å for DPhO-PPh and $c = 49.5 \pm 0.5$ Å for DPhO-2,5PRM. Structure organization of such densely packed chains which have a substantial conformation freedom or conformation disordering have neither amorphous nor ordered crystalline regions. It can be classified as the 'conformation disordered crystals' following Wunderlich [32]. The X-ray patterns of the coPI fibres that were studied have no (*hkl*) reflections which correspond to the three-dimensional order. Lack of these reflections make it possible to conclude that there is a one phase, mesomorphic structure in the coPI fibres. The coPI macromolecules pass from one microblock to another, that does not result in an essential change in the lattice parameters or in chain breaks between the blocks. Such a supermolecular structure explains the high density of coPI fibres $\rho = 1.45–1.49$ g/sm^3 and its high thermostability [28].

The analysis of the mechanical properties of the PI fibres studied show that the highest determined value of strength is 3.0 ± 0.2 GPa for coPI fibre with a composition of 50/50 as compared to the homoPI values of DPhO-PPh (1.0 ± 0.1 GPa) and DPhO-2,5PRM (1.5 ± 0.3 GPa). Thus, from mechanical testing, the coPI fibre with an apparently high strength was made. It should be noted that the maximum modulus 130 GPa was also obtained for the coPI fibre with a composition of 50/50.

The comparison of modulus and strength of the homoPI and coPI fibres studied shows that the coPI fibres with the composition 50/50 and 60/40 have higher values than those for homoPI. Its modulus is about 1.5 times greater and strength 3 times greater than those of the DPhO-PPh homoPI. The values of ductility, as measured by the elongation to break, for the coPI fibre (3.3%) are greater than for DPhO-PPh homoPI (1.2%) and for DPhO-2,5PRM homoPI (2.0%).

The correlation of structure and morphology to properties of homoPI and coPI fibres can be discussed, using previous results. The 'bulk' tensile fibre modulus of the DPhO-PPh homoPI fibre, as measured by mechanical testing, is about 91 GPa, while the lattice modulus, as determined by WAXD, is about 210 GPa [1]. The lower value of 'bulk' modulus compared with the lattice modulus suggests a number of unoriented regions and disordered molecules in this fibre. Electron microscopical data show that this fibre has a feasible skin about 4 μm thick with large pores and a more dense core with small pores which dramaticaly reduced the strength of the fibre. The low modulus of the fibre, as compared with the lattice modulus, can be explained by the low degree of molecular orientation along the fibre axis and by the mesomorphic type of the molecular packing.

In this investigation, the intrinsic viscosity of PAA and coPAA solutions, during the preparation of fibres, ranges from $[\eta] = 2.8$ to 3.2 dl/g. The improvement in tensile fibre properties of coPI fibres cannot be explained by the big difference in the intrinsic viscosity and, therefore, in the molecular weights between the homo- and coPI used in this case.

The increase in the strength (3.0 GPa) and modulus (130 GPa) of coPI with the composition 50/50 when compared with the strength and modulus of the homoPI (1.0 and 91 GPa for DPhO-PPh, 1.5 and 118 GPa for DPhO-2,5PRM) significantly exceed the values predicted by the 'rule of mixtures' [33]. Synergism of properties can be explained in the context of the occurrence of the microblock structure and a specific composed morphology in the coPI fibres. Improvement of mechanical properties identical to that was observed for chemically similar coPI fibres prepared by wet-spinning into a coagulation bath consisting of ethanol:glycol = 1:1 [28], as well as it has been reported by us [19,23,34] for coPI fibres based on the pyromellitic dianhydride with rigid and flexible diamines with the mole ratio 60/40 and 50/50.

5. Conclusions

It was shown that the fibrillar structure of PI fibres studied differ substantially from that in the semi-crystalline polymers. Various morphological organizations, depending on the chemical structure, the flexibility of homoPI chains and the composition of coPI fibres were observed under the same preparation conditions.

DPhO-PPh fibre is composed of spindle-shaped short fibrils about 30–60 nm in diameter. The fibre exhibits a skin-core morphology with a feasible porous skin of 2-4 μm thickness and a more dense core. The fibre has the mesomorphic texture with the axis coinciding with the fibre axis. Strong reflections responsible for the 3-D order in fibre are absent. The fibre is very brittle.

DPhO-2,5PRM fibre has fibrillar bundles, which consist of ribbon-like fibrils with a thickness of about 20 nm and a width ranging from 30 nm to a few micrometers. The fibre did not show the pronounced skin–core effect, but the surface looks less ordered (thin layer not more than 0.5 μm in thickness). The fibre exhibits the mesomorphic structure with the higher degree of chain orientation and less dense mutual packing of the macromolecules than the previous one.

However, the coPI fibres with the compositions 50/50 and 60/40 exhibit the highest strength, high elastic modulus in combination with high elongation at break. These coPI fibres have the fibrillar core and the homogeneous skin about 1 μm thick. Improvement in the mechanical properties of coPI fibres can be explained by the occurrence of the microblock structure on the X-ray level, the 'strand of

beads' fibrils and composed 'skin-core' morphology with the radial heterogeneity on the macro level.

Acknowledgements

We are grateful to Dr. G.M. Mikhailov, Mrs. N.V. Bobrova and Dr. V.E. Yudin for the preparation, supply and mechanical testing of the PI fibre samples, as well as for a fruitful discussion.

References

[1] Bessonov MI, Koton MM, Kudryavtsev VV, Laius LA. Polyimides: thermally stable polymers. New York: Plenum Press, 1987.
[2] Yang HH. Aromatic high-strength fibres. New York: Wiley, 1989.
[3] Sroog CE. Polyimides. Prog Polym Sci 1991;16:561.
[4] Weinrotter K, Seidl S. High-performance polyimide fibers. In: Lewin M, Preston J, editors. High technology fibers, Part C, New York: Marcel Dekker, 1993. p. 179, Ser. 3.
[5] Polyimides. In: Mittal KL, editor. New York: Plenum Press, 1984.
[6] Irwin RS. US Pat 3 415 782, E.I. duPont & Co, 1968.
[7] Irwin RS. US Pat 4 640 972, E.I. duPont & Co, 1987.
[8] Koton MM. Br Pat 1 183 306, 1970.
[9] Koton MM. Br Pat 2 025 311, 1980.
[10] Prokopchuk NR, Baklagina YG, Korzhavin LN, Sidorovich AV, Koton MM. Vysokomol Soedin 1977;A19:1126.
[11] Prokopchuk NR, Korzhavin LN, Sidorovich AV, Milevskaya IS, Baklagina YG, Koton MM. Dokl Akad Nauk SSSR 1977;236:127.
[12] Jinda T, Matsuda T, Sakamoto M. Sen-i-Gakkaishi 1984;40(12):480.
[13] Jinda T, Matsuda T. Sen-i-Gakkaishi 1986;42(10):554.
[14] Kaneda T, Katsura T, Nakagawa K, Makino H, Horio M. J Appl Polym Sci 1986;32:3133–3151.
[15] Hara S, Yamada T, Yoshida T. US Pat 3 829 399, 1974.
[16] Minami M, Taniguchi M. US Pat 3 860 559, 1975.
[17] Nagaoka K. US Pat 4 448 957 1984.
[18] Du Pont. Kevlar, Du Pont Engineering Fibres, Geneva, Brochure H-22999, 1993. p. 26.
[19] Baklagina Yu G, Sklizkova VP, Mikhailov GM, Kudryavtsev VV, Sukhanova TE, Sidorovich AV. Izvestya Academii Nauk SSSR 1991;55:1763.
[20] Baklagina YG, Milevskaya IS. Supermolecular structure of polyamic acids and polyimides. In: Bessonov MI, Zubkov VA, editors. Polyamic acids and polyimides: synthesis, transformations and structure, Boca Raton: CRC Press, 1993. p. 197.
[21] Baklagina YG, Lukasheva NV, Artem'eva VN, Sklizkova VP, Lavrentjev VK, Denisov VM, Mikhailov GM, Kudryavtsev VV, Kalbin AG. A model of supermolecular structure for aromatic polyimide copolymers and blends with chains of various rigidities. In: Feiger C, editor. Advances in polyimide science and technology, 1991. p. 405.
[22] Milevskaya IS, Baklagina YuG, Sidorovich AV, Korzhavin LN, Lukasheva NV. Zh Strukt Khim 1981;22:42.
[23] Sukhanova TE, Baklagina YG, Mikhailov GM, Sklizkova VP, Kudryavtsev VV. Proc 10th European Congress on Electron Microscopy, vol. 2. Granada, Spain: EUREM 92, 1992. p. 467.
[24] Sukhanova TE, Lednicky F. Proc 13th International Congress on Electron Microscopy, vol. 2, 1994. p. 517.
[25] Olley RH, Basset DS. Polymer 1982;23:1707.
[26] Sukhanova TE, Lednicky F, Urban J, Baklagina YG, Mikhailov GM, Kudryavtsev VV. J Mater Sci 1995;30:2201.
[27] Dobb MG, Johnson DJ, Saville BP. Polymer 1981;22:960.
[28] Mikhailov GM, Korzhavin LN, Kudryavtsev VV, Koton MM, Maricheva TA, Ivanova MA, Bobrova NV, Bronnikov SV, Grigorjeva NA, Shkurko OP, Borovik VP, Yakopson SM, Karchmarchik O.S. RU Pat 2 062 276 1996.
[29] Artem'eva VN, Kudryavtsev VV, Nekrasova EM, Sklizkova VP, Baklagina YuG, Lukasheva NV, Shkurko OP, Borovik VP. Izv Akad Nauk Khim Ser 1992;10:2288.
[30] Waddon AJ, Karasz FE. Polymer 1992;33:3783.
[31] Livingston HK. J Polym Sci Part C 1967;18:105.
[32] Wunderlich B, Grebowicz J. ACS Polym Prepr 1983;24:290.
[33] Hwang W-F, Wiff DR, Benner CL, Helminiak TEJ. Macromol Sci Phys 1983;B22:231.
[34] Mikhailov GM, Bobrova NV, Lebedeva MF, Baklagina YuG, Maricheva TA, Sukhanova TE. Zh Prikl Khim 1994;67:2027.